CONFIDENTIAL

Copy
RM L56H24

C2

NACA

RESEARCH MEMORANDUM

COMBINED EFFECTS OF WING TAPER RATIO AND LOW HORIZONTAL-TAIL POSITION ON LONGITUDINAL STABILITY OF A 45° SWEPTBACK WING-BODY COMBINATION AT TRANSONIC SPEEDS

By Stanley H. Spooner

Langley Aeronautical Laboratory
Langley Field, Va.

CLASSIFIED DOCUMENT

NATIONAL ADVISORY COMMITTEE
FOR AERONAUTICS

WASHINGTON

October 31, 1956

CONFIDENTIAL

NACA RM L56H24

NATIONAL ADVISORY COMMITTEE FOR AERONAUTICS

RESEARCH MEMORANDUM

COMBINED EFFECTS OF WING TAPER RATIO AND LOW HORIZONTAL-TAIL POSITION ON LONGITUDINAL STABILITY OF A 45° SWEPTBACK WING-BODY COMBINATION AT TRANSONIC SPEEDS

By Stanley H. Spooner

SUMMARY

The combined effects of wing taper ratio and low horizontal-tail position on the static longitudinal stability of a 45° sweptback wing-body combination with an aspect ratio of approximately 4 have been investigated for a range of Mach numbers from 0.8 to 1.2 in the Langley 8-foot transonic pressure tunnel.

The initial destabilizing tendency exhibited by the wing-fuselage combination is reduced as the wing taper ratio is decreased from 0.31 to 0. The addition of a horizontal tail in a low position does not eliminate this destabilizing tendency. Although the horizontal tail contributes to the stability at all Mach numbers and angles of attack investigated, the amount of the horizontal-tail contribution decreases as the wing taper ratio is decreased. Large stability changes with Mach number occur for all configurations.

INTRODUCTION

It is advantageous from a standpoint of drag due to lift for wings to have high aspect ratios. Some sweptback wings with high aspect ratios, however, have exhibited undesirable pitch-up tendencies. Previous investigations have shown that by reducing the taper ratio of such wings, the pitch-up tendencies can be reduced and, in some cases, eliminated. Furthermore, it has been found that a horizontal tail mounted below the extended wing chord plane can also alleviate the pitch-up problem. The separate effects of taper ratio and low tail position on some sweptback wings have been reported for the low subsonic speed range (ref. 1) and to some extent, for the high subsonic speed range. (See refs. 2 and 3.)

The investigation reported herein shows the combined effects of taper ratio and low tail position on the static longitudinal stability of a series of wings having 45° sweepback and aspect ratio of approximately 4. The lift and pitching-moment characteristics are presented for an angle-of-attack range of approximately -2° to 20° and a Mach number range of 0.8 to 1.2.

SYMBOLS

C_L	lift coefficient, $\frac{\text{Lift}}{qS_w}$
C_m	pitching-moment coefficient, about $0.25\bar{c}_w$, $\frac{\text{Pitching moment}}{qS_w\bar{c}_w}$
q	free-stream dynamic pressure, lb/sq ft
S	area, sq ft
$\bar{c}$	mean aerodynamic chord, $\frac{2}{S}\int_0^{b/2} c^2 dy$, ft
c	local chord, ft
b	wing span, ft
y	spanwise distance from plane of symmetry, ft
x	chordwise distance from leading edge of mean aerodynamic chord to neutral point, positive rearward, ft
λ	taper ratio
M	free-stream Mach number
α	angle of attack, deg
i_t	angle of incidence of horizontal tail with respect to the wing chord, deg
V_t	tail volume coefficient, $\frac{l}{\bar{c}_w}\frac{S_t}{S_w}$

[redacted]

l distance from $0.25\bar{c}_w$ to $0.25\bar{c}_t$, ft

z perpendicular distance between wing and tail chord planes, measured with $i_t = 0^\circ$

$\partial\epsilon/\partial\alpha$ rate of change of downwash angle at horizontal tail with angle of attack

$C_{L_{\alpha_t}}$ lift-curve slope of horizontal tail

$C_{m_{C_L}}$ static-longitudinal-stability parameter

$C_{m_{i_t}}$ rate of change of pitching-moment coefficient with horizontal-tail incidence

C_{m_t} pitching-moment coefficient contributed by horizontal tail

τ tail stability parameter

Subscripts:

w wing

t tail

e effective

MODELS

The principal dimensions of the models are shown in figure 1. The geometry of the models is shown in table I. The wings had a quarter-chord sweepback angle of 45°, NACA 65A006 airfoil sections, and an aspect ratio of approximately 4. The only differences in the wings were the taper ratios which were 0, 0.16, and 0.31. The wings were mounted in a midwing position on the body.

The horizontal tail had the same aspect ratio, sweepback, and airfoil sections as the wings but had a taper ratio of 0.6. The tail area was about 25 percent of that for the wings. The tail-length ratios $l/\bar{c}_w$ of the three wing configurations were not the same because of the different mean-aerodynamic-chord lengths. The horizontal tail was mounted 0.054 wing semispan below the extended wing chord plane for each wing-body configuration.

[redacted]

The bodies were indented in the region of the wing and had a fineness ratio of approximately 11.5. The wing with a taper ratio of 0.31 was of solid aluminum alloy; the wings with taper ratios of 0 and 0.16, as well as the horizontal tail and the body structure, were of steel. The external surfaces of the bodies were constructed of fiber glass and plastic.

APPARATUS AND TESTS

The tests were conducted in the Langley 8-foot transonic pressure tunnel. The forces and moments were measured simultaneously by means of an electrical strain-gage balance mounted within the models. The angle of attack was measured by means of an electrical strain-gage pendulum device also mounted within the models.

All tests were made with the air in the tunnel at a stagnation pressure of one atmosphere and a stagnation temperature of about 124° F. The Mach number range extended from 0.8 to 1.2. The variation of Reynolds number, based on $\bar{c}_w$, with Mach number is shown in figure 2. The angle-of-attack range extended from a small negative angle to the maximum angle allowed by the balance load limits and the tunnel power.

A tail-off and a tail-on test run at each of two tail incidences (0°, -4°) were made through the angle-of-attack and the Mach number range for each wing-body combination.

REDUCTION OF DATA

All data have been reduced to standard nondimensional coefficients. Jet-boundary and blockage corrections are negligible and have not been applied to the data. At the Mach numbers for which the data are presented, the effects of the boundary-reflected disturbances are also negligible. Although the effects of the aeroelastic properties of the models were not determined, it is believed that, if an account were made for these effects, the trends indicated herein would be substantially the same.

The effective downwash angle and the dynamic-pressure ratio are calculated from the experimental pitching-moment data. In the computation of the effective dynamic-pressure ratio, the following equation was used:

$$\left(q_t/q\right)_e = - \frac{C_{m_{i_t}}}{C_{L_{\alpha_t}} V_t} \tag{1}$$

in which the values of $C_{L_{\alpha_t}}$ were determined from the data presented in reference 4 and shown in figure 3 for a wing of similar geometry as the horizontal tail but mounted in a midwing position on a body of circular cross section. The effect of the fuselage on the tail efficiency, therefore, is included in $C_{L_{\alpha_t}}$ and is assumed to be the same for the lower tail position on the fuselage used in the tests reported herein.

The combined effects of downwash angle and dynamic pressure on the stabilizing contribution of the horizontal tail are defined by the tail stability parameter τ. The values presented herein were computed according to the equation given in reference 5:

$$\tau = \frac{\partial C_{m_t}}{\partial \alpha} \frac{1}{C_{L_{\alpha_t}} V_t} \tag{2}$$

In the determination of $(\partial\epsilon/\partial\alpha)_e$, $\left(q_t/q\right)_e$, and τ, the assumption is made that the tail lift curve is linear. As shown in reference 4, the lift curves are essentially linear up to an angle of about 8°. The values of $(\partial\epsilon/\partial\alpha)_e$, $\left(q_t/q\right)_e$, and τ, therefore, are not presented herein for those conditions at which the angle of attack of the tail is calculated to exceed 8°.

ACCURACY

The average free-stream Mach number is estimated to be accurate within ±0.003. The estimated accuracy of the angle of attack and the coefficients based on previous tests, is as follows:

α, deg	±0.1
C_L	±0.02
C_m	±0.004

[redacted]

RESULTS AND DISCUSSION

The lift and pitching-moment characteristics of the wing-fuselage combinations without the horizontal tail are shown in figures 4 to 6. The tail-on characteristics are shown in figures 7 to 10 for tail incidences of -4° and 0°. The variation of the flow parameters $(\partial\epsilon/\partial\alpha)_e$ and $\left(q_t/q\right)_e$ and the tail stability parameter τ with angle of attack and with Mach number is shown in figures 11 and 12, respectively.

Tail-Off Pitch Characteristics

The wing-body combination with taper ratio of 0.31 shows pitching-moment characteristics similar to those obtained previously with wings having similar sweepback and aspect ratio. Namely, the stability parameter $C_{m_{C_L}}$, as shown in figure 5, has a constant value or becomes slightly more negative as the lift coefficient increases through the low lift range. A destabilizing tendency then occurs, followed by an abrupt pitch-down tendency.

As the taper ratio decreases from 0.31 to 0, the magnitude of the destabilizing tendency becomes smaller but occurs initially at a lower lift coefficient. These effects have been noted previously in reference 2, for example, for 45° sweptback wings having taper ratios of 0.30, 0.60, and 1.00.

The variation of the stability parameter $C_{m_{C_L}}$ with Mach number for several lift coefficients is shown in figure 6. In general, the overall trend at all lift coefficients is for a change in $C_{m_{C_L}}$ with increase in Mach number corresponding to a rearward movement of the aerodynamic center. The variation of $C_{m_{C_L}}$ with Mach number is slightly erratic at low lift coefficients and much more so at the higher lift coefficients for Mach numbers between 0.90 and 1.00. For example, at a lift coefficient of 0.6, the change in the value of $C_{m_{C_L}}$ for the wing with taper ratio of 0.31 between Mach numbers of 0.94 and 0.98 corresponds to a rearward movement of the aerodynamic-center location of 23 percent of the mean aerodynamic chord. Reduction of the wing taper ratio from 0.31 to 0 reduces the change in $C_{m_{C_L}}$ with Mach number but does not eliminate it.

Tail-On Pitch Characteristics

The static longitudinal stability of the wing-body combinations with the horizontal tail mounted 0.054b/2 below the extended wing chord plane is illustrated in terms of neutral-point location in figures 9 and 10. The variation of the neutral-point location with lift coefficient or Mach number is similar to the variation of the stability parameter $C_{m_{C_L}}$ obtained with the tail-off configurations shown in figures 5 and 6. The initial destabilizing tendency which occurs at moderate lift coefficients is not eliminated by the addition of the horizontal tail. At higher lift coefficients, stability changes with lift coefficient occur which correspond to rearward shifts of the neutral point exceeding 50 percent of the mean aerodynamic chord. Stability changes with Mach number occur at high lift coefficients which correspond to movements of the neutral point exceeding 25 percent of the mean aerodynamic chord.

A somewhat lower tail position or the incorporation of negative dihedral in the tail might eliminate completely the unstable tendency of the wing-body combinations. The advantage of using negative dihedral or a low tail position, on the basis of tests made at low subsonic speeds, is reported in reference 1. The favorable effects at higher speeds of low tail position are reported in reference 3.

Effective Flow Characteristics Over Horizontal Tail

Variation with angle of attack.- The variation of the longitudinal stability parameters $(\partial\epsilon/\partial\alpha)_e$ and $\left(q_t/q\right)_e$ with angle of attack is shown in figure 11. In the low angle-of-attack range, the values of $(\partial\epsilon/\partial\alpha)_e$ and $\left(q_t/q\right)_e$ remain nearly constant. At high angles of attack for almost all Mach numbers, a rapid decrease in the values of $(\partial\epsilon/\partial\alpha)_e$ occurs.

Above the angle of attack corresponding to that at which the initial instability occurs, the value of $\left(q_t/q\right)_e$ increases rapidly with increasing angle up to the angle at which the abrupt pitch-down tendency is reached. Above this angle, $\left(q_t/q\right)_e$ rapidly decreases.

Reduction of the taper ratio from 0.31 to 0 results in an increase in the values of $(\partial\epsilon/\partial\alpha)_e$ at most angles of attack. As has been mentioned, a reduction in taper ratio resulted in a reduction of the tail-length ratio $l/\bar{c}_w$. It is believed that the effect of the change in

tail-length ratio is not significant and that the changes in $(\partial\epsilon/\partial\alpha)_e$ can be attributed to the changes in the wing taper ratios.

The combined effects of downwash angle and dynamic pressure on the stabilizing contribution of the tail are shown in figure 11 by the parameter τ. As indicated by the negative values of the parameter τ, the tail contributes to the stability throughout the angle-of-attack range investigated. At low angles of attack, τ remains essentially constant for the wing with taper ratio of 0 and varies somewhat for the other wing configurations. At about 10° to 12° and for all configurations, the tail contribution rapidly increases with increase in angle of attack. At the higher Mach numbers, the stability contribution by the horizontal tail varies erratically with angle of attack in a manner similar to that obtained for the variation of $(\partial\epsilon/\partial\alpha)_e$ with angle of attack. In general, the contribution of the tail to the stability, as indicated by the parameter τ, decreases as the wing taper ratio decreases.

Variation with Mach number.- The variation of $(\partial\epsilon/\partial\alpha)_e$ and $\left(q_t/q\right)_e$ with Mach number is shown in figure 12. At the lower lift coefficients, $(\partial\epsilon/\partial\alpha)_e$ generally increases to a maximum value between Mach numbers of 0.94 and 0.98 and then decreases with increase in Mach number. The minimum value of $\left(q_t/q\right)_e$ occurs between Mach numbers of 0.90 to 0.94. The variation with Mach number of the combined effects is also shown in figure 12. The tail contribution to the stability generally decreases with increase in Mach number and reaches a minimum value between Mach numbers of 0.90 and 0.98. From these Mach numbers to a Mach number of 1.03, the parameter τ rapidly becomes more negative. For a Mach number of 1.2, the contribution of the tail becomes greater with increase in Mach number for low lift coefficients and remains about constant or decreases at higher lift coefficients.

In general, for the Mach number range investigated, the flow is such that the horizontal tail contributes least to the stability of the taper ratio 0 wing-body combination and most to the taper ratio 0.31 wing-body combination.

CONCLUSIONS

From the results of wind-tunnel tests in the Langley 8-foot transonic pressure tunnel of the combined effects of taper ratio and low horizontal-tail position on the static longitudinal stability of a 45° sweptback wing-body combination with an aspect ratio of approximately 4, the following conclusions may be drawn:

[redacted]

1. The initial destabilizing tendency exhibited by the wing-fuselage combinations is reduced, but not eliminated, as the wing taper ratio is decreased from 0.31 to 0. The addition of the horizontal tail does not eliminate the initial destabilizing tendency.

2. The flow characteristics at the horizontal tail are such that the contribution of the tail to the stability decreases as the wing taper ratio decreases from 0.31 to 0. The horizontal tail, however, contributes to the stability at all Mach numbers and angles of attack.

3. Stability changes with Mach number which correspond to shifts of the neutral point exceeding 25 percent of the mean aerodynamic chord occur for all configurations.

Langley Aeronautical Laboratory,
National Advisory Committee for Aeronautics,
Langley Field, Va., August 8, 1956.

[redacted]

REFERENCES

1. Neely, Robert H., and Griner, Roland F.: Summary and Analysis of Horizontal-Tail Contribution to Longitudinal Stability of Swept-Wing Airplanes at Low Speeds. NACA RM L55E23a, 1955.

2. King, Thomas J., Jr., and Pasteur, Thomas B., Jr.: Wind-Tunnel Investigation of the Aerodynamic Characteristics in Pitch of Wing-Fuselage Combinations at High Subsonic Speeds - Taper-Ratio Series. NACA RM L53E20, 1953.

3. Silvers, H. Norman, and King, Thomas J., Jr.: Investigation at High Subsonic Speeds of the Effect of Horizontal-Tail Location on Longitudinal and Lateral Stability Characteristics of a Complete Model Having a Sweptback Wing in a High Location. NACA RM L56B10, 1956.

4. Osborne, Robert S., and Mugler, John P., Jr.: Aerodynamic Characteristics of a 45° Sweptback Wing-Fuselage Combination and the Fuselage Alone Obtained in the Langley 8-Foot Transonic Tunnel. NACA RM L52E14, 1952.

5. Foster, Gerald V., and Griner, Roland F.: Low-Speed Longitudinal and Wake Air-Flow Characteristics at a Reynolds Number of 5.5×10^6 of a Circular-Arc 52° Sweptback Wing With a Fuselage and a Horizontal Tail at Various Vertical Positions. NACA RM L51C30, 1951.

TABLE I.- SUMMARY OF GEOMETRIC CHARACTERISTICS OF WINGS AND TAIL

	Wings			Tail
Taper ratio	0	0.16	0.31	0.60
Aspect ratio	4.00	3.94	3.90	4.00
Area, sq in.	129.384	131.278	132.667	32.832
Span, in.	22.750	22.750	22.750	11.460
Mean aerodynamic chord, in.	7.583	6.790	6.368	2.921
Sweepback, deg	45	45	45	45
Airfoil section	NACA 65A006	NACA 65A006	NACA 65A006	NACA 65A006
S_t/S_w	0.254	0.250	0.248	
$l/\bar{c}_w$	1.808	2.018	2.153	
V_t	0.459	0.504	0.534	
$2z/b_w$	-0.054	-0.054	-0.054	
Body fineness ratio	11.3	11.4	11.7	

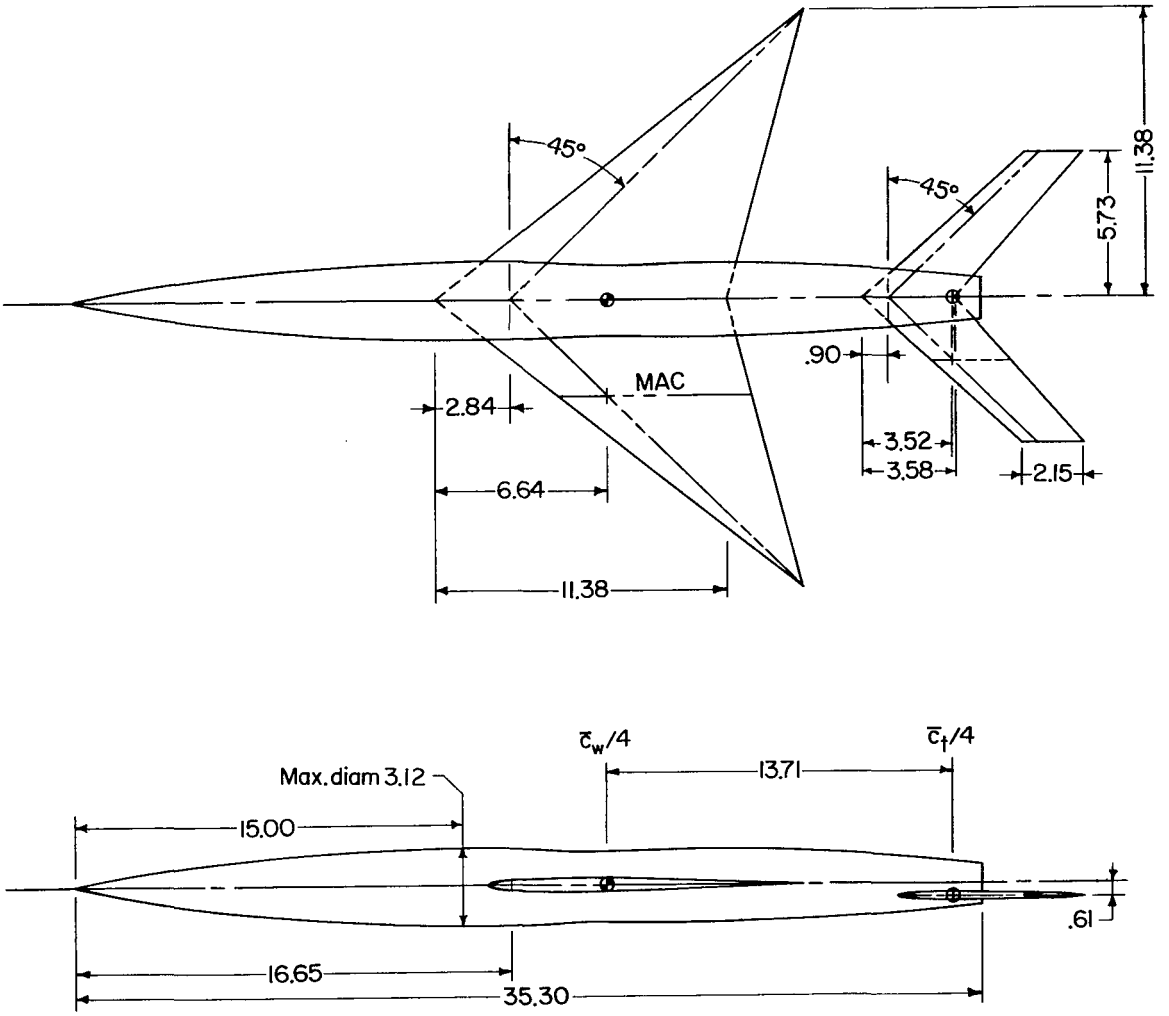

(a) $\lambda = 0.$

Figure 1.- Principal dimensions of models. (All linear dimensions in inches.)

[redacted]

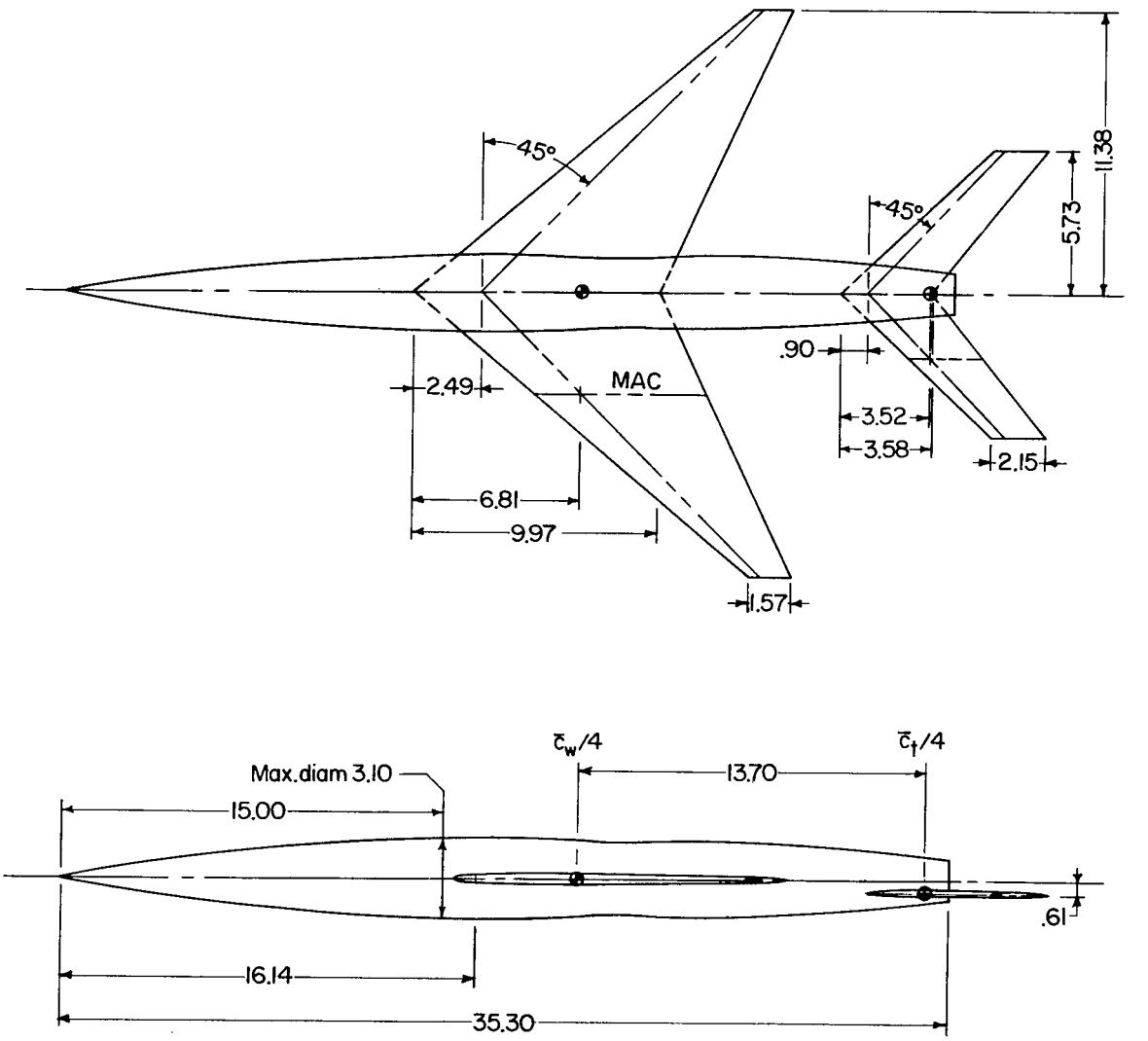

(b) $\lambda = 0.16$.

Figure 1.- Continued.

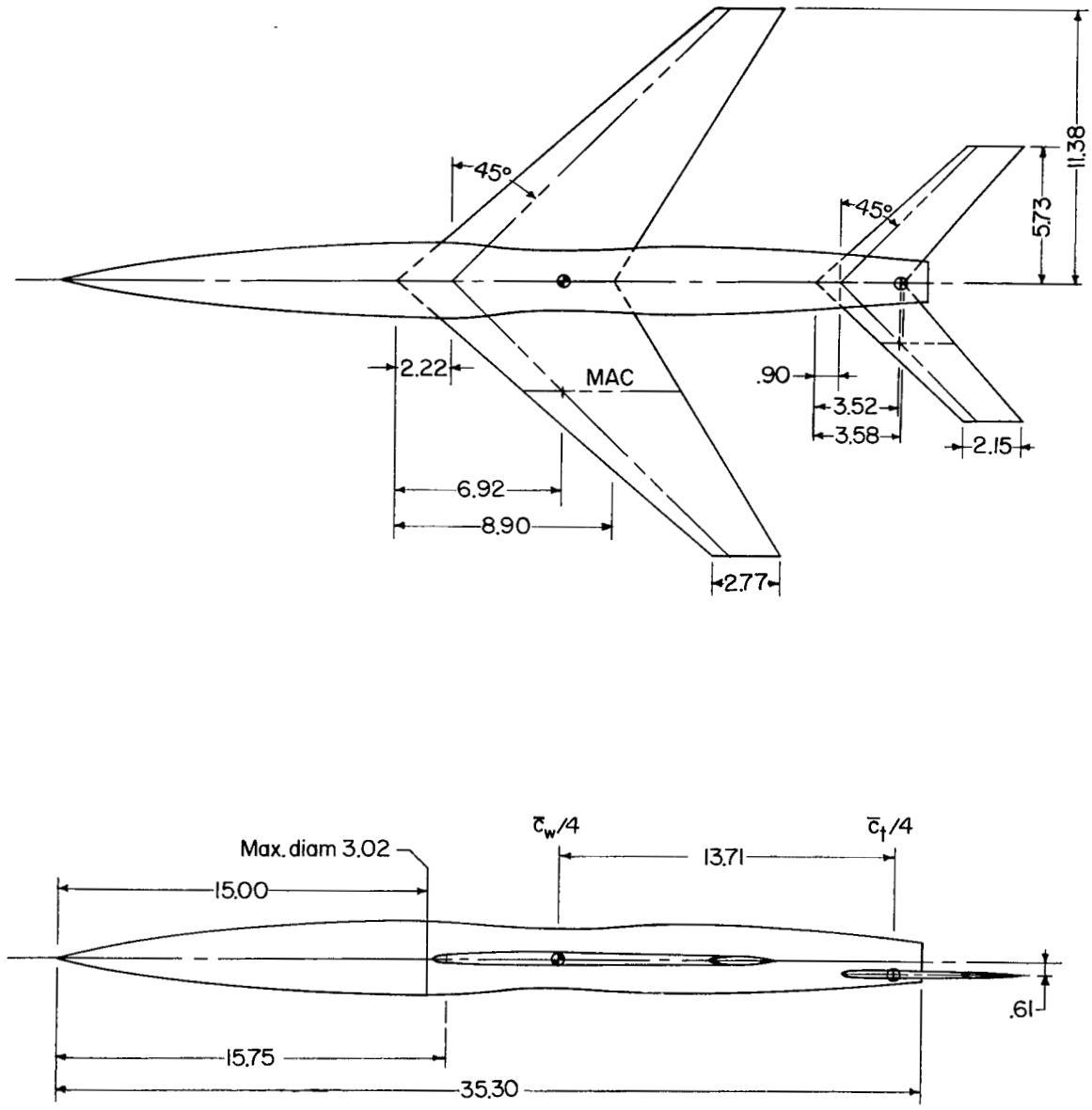

(c) $\lambda = 0.31$.

Figure 1.- Concluded.

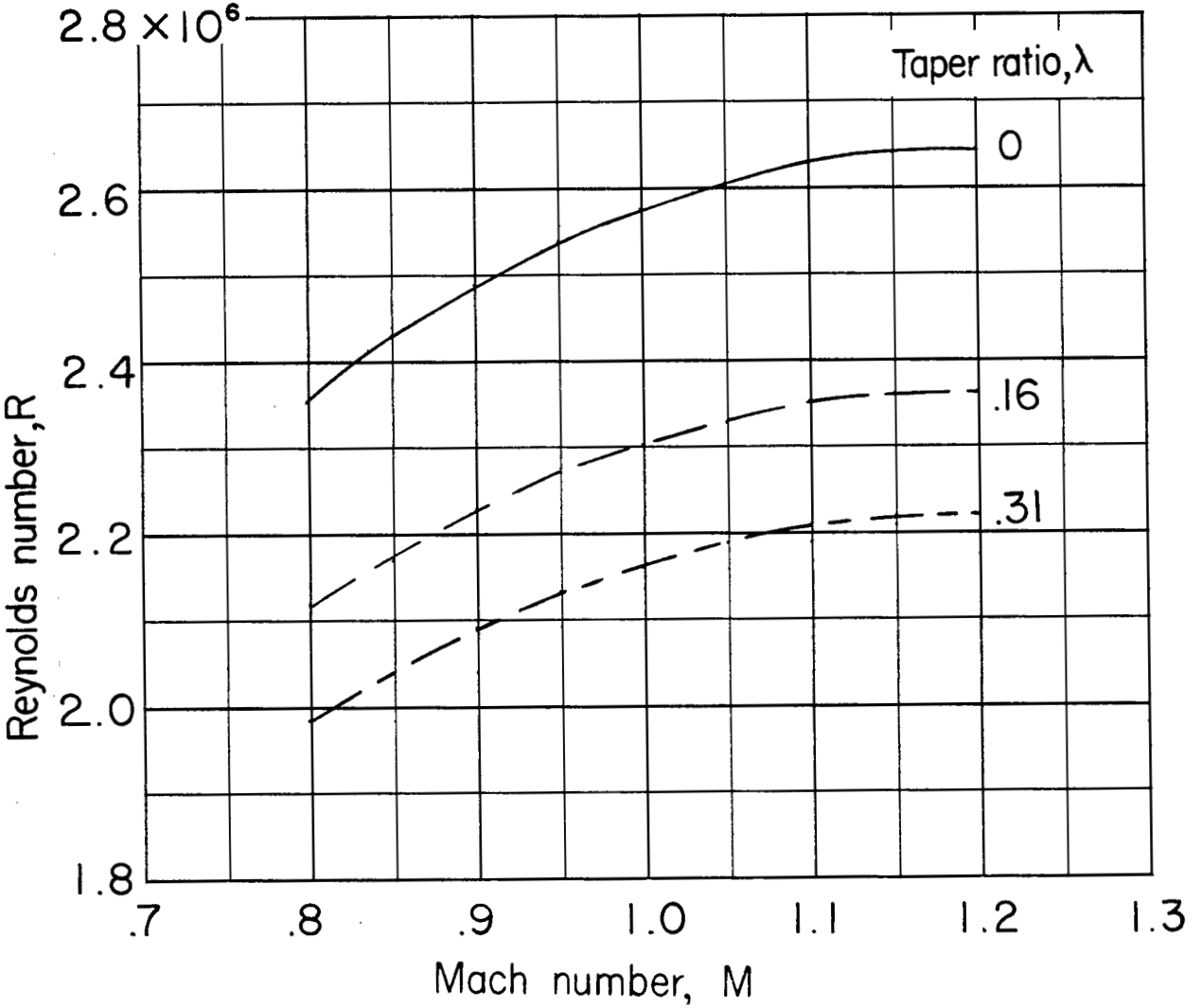

Figure 2.- Variation of Reynolds number, based on $\bar{c}$, with Mach number.

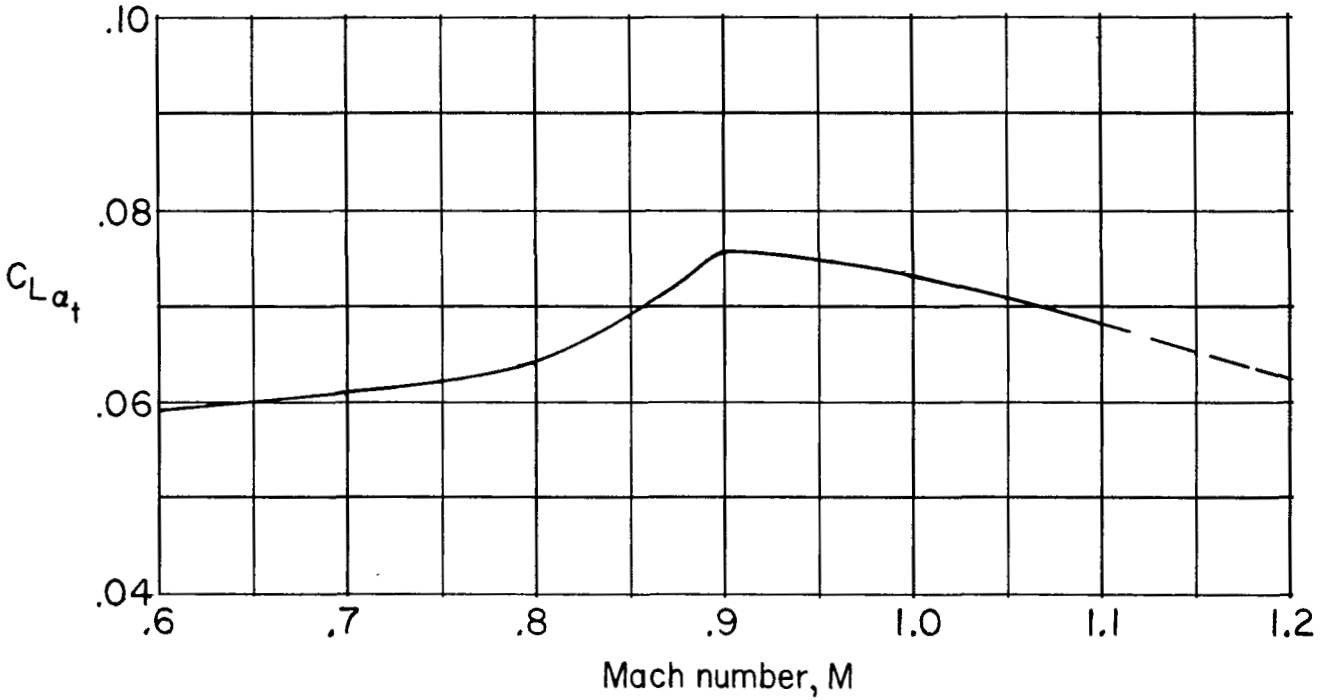

Figure 3.- Variation of $C_{L_{\alpha_t}}$ with Mach number; obtained from reference 4.

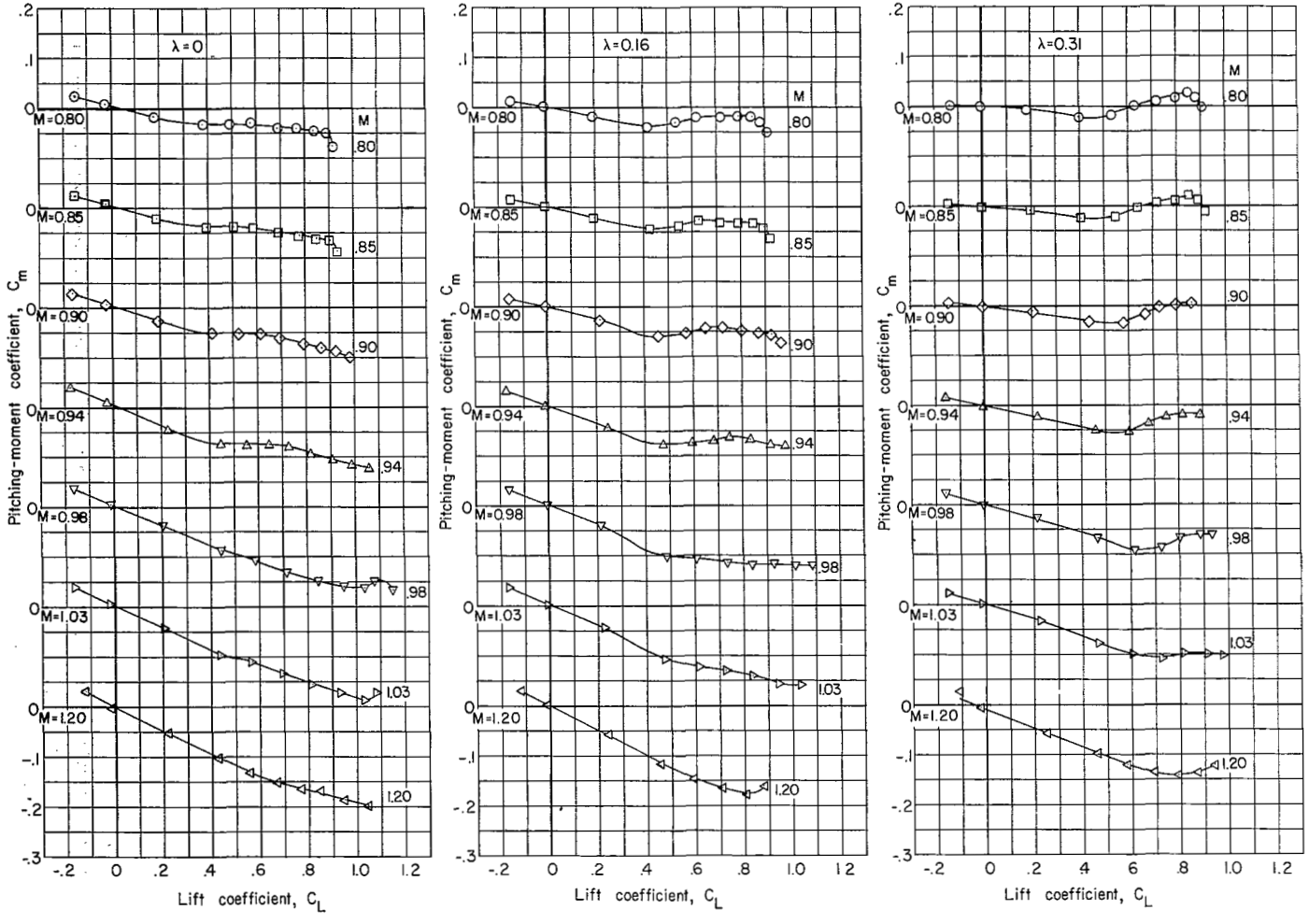

(a) Pitching moment.

Figure 4.- Aerodynamic characteristics of the wing-body combinations.

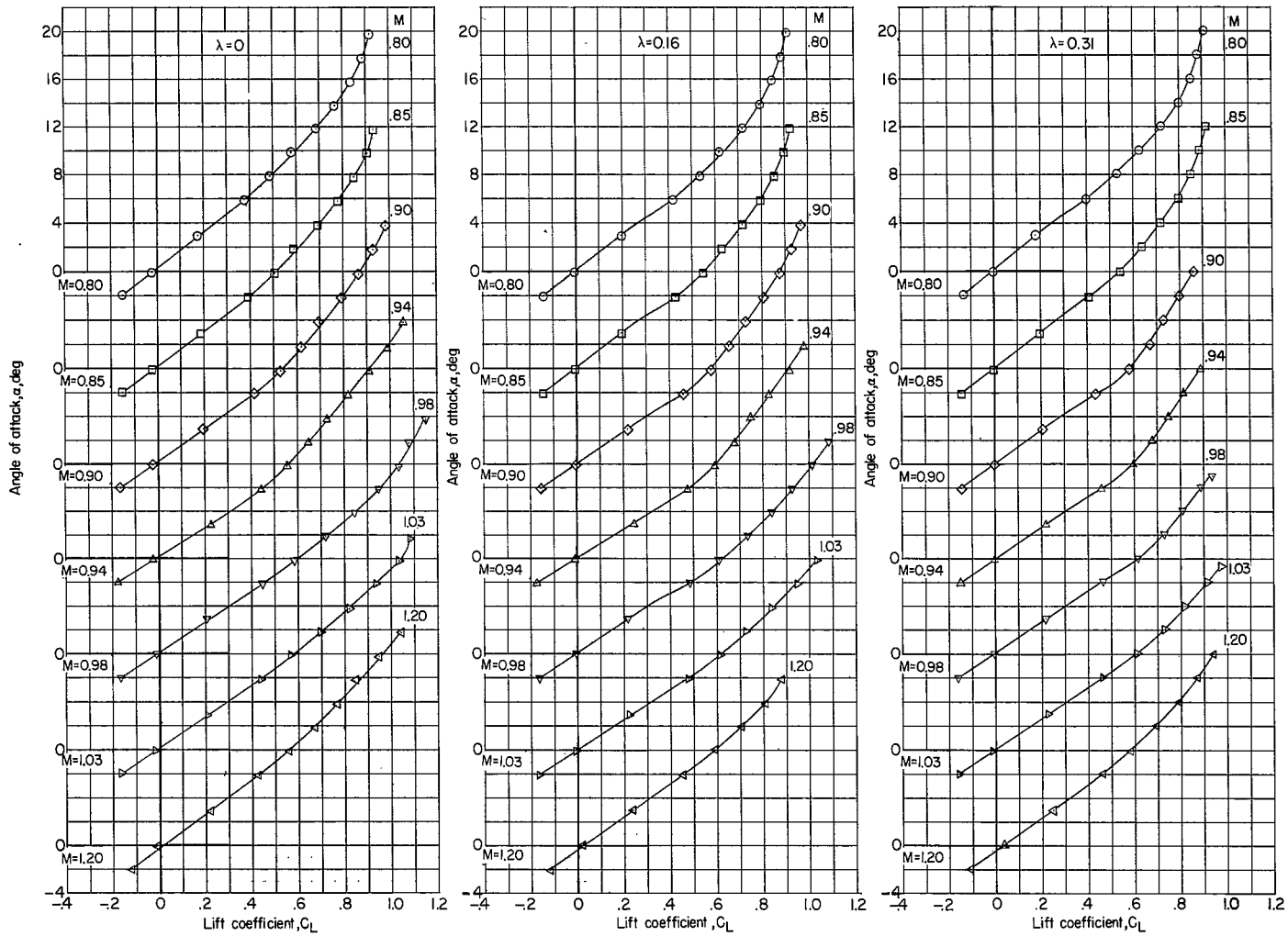

(b) Lift.

Figure 4.- Concluded.

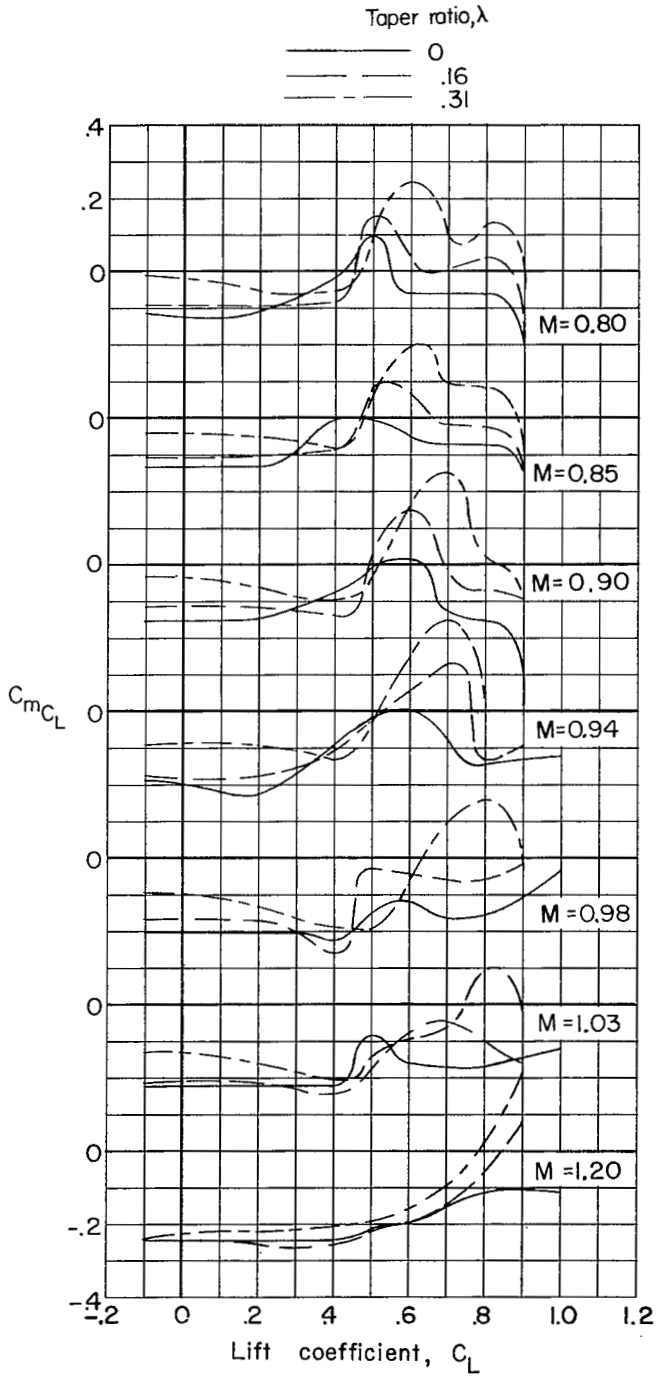

Figure 5.- Variation of the stability parameter $C_{m_{C_L}}$ with lift coefficient for the wing-body combinations.

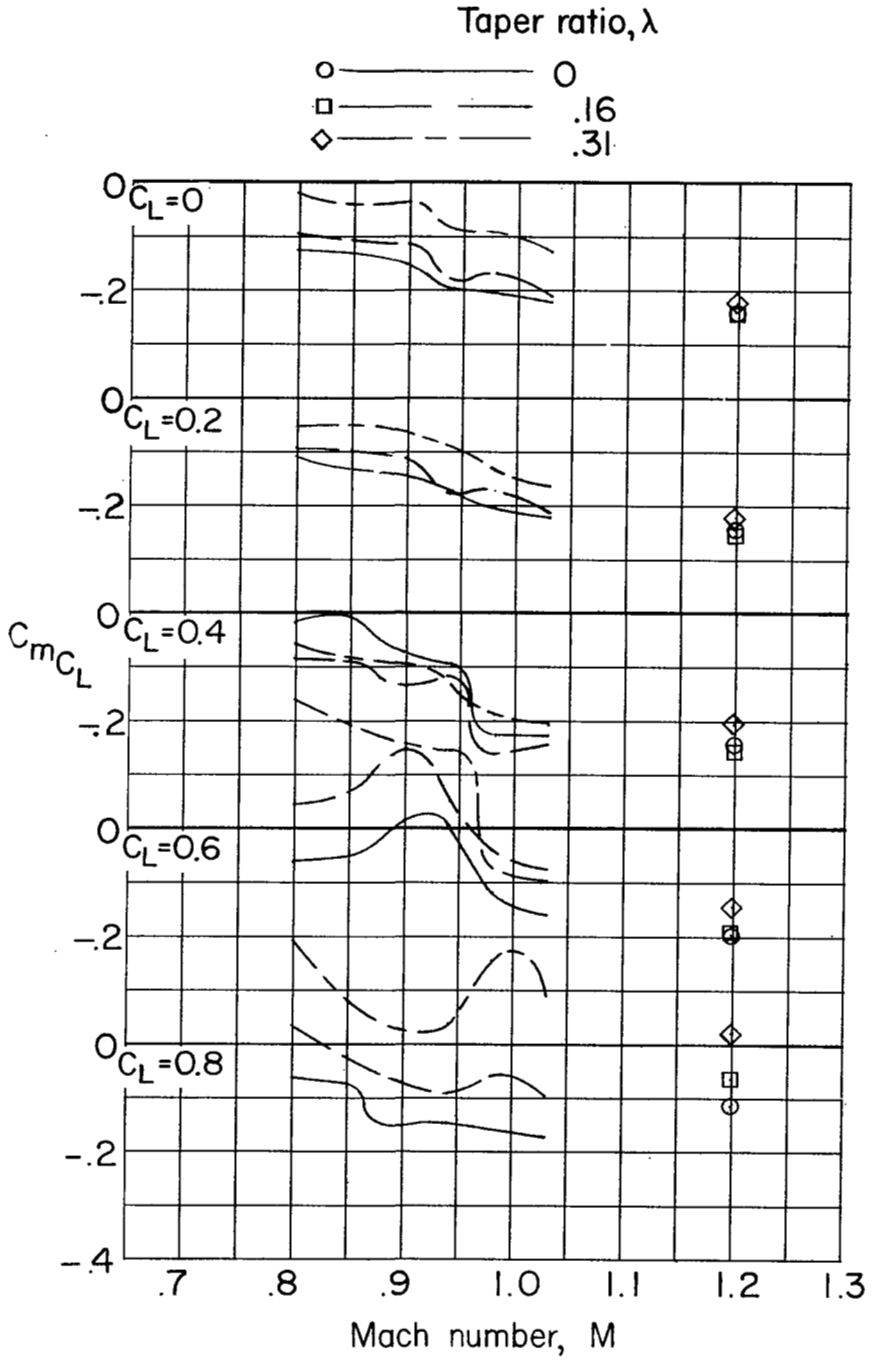

Figure 6.- Variation of the stability parameter $C_{m_{C_L}}$ with Mach number for the wing-body combinations.

[redacted]

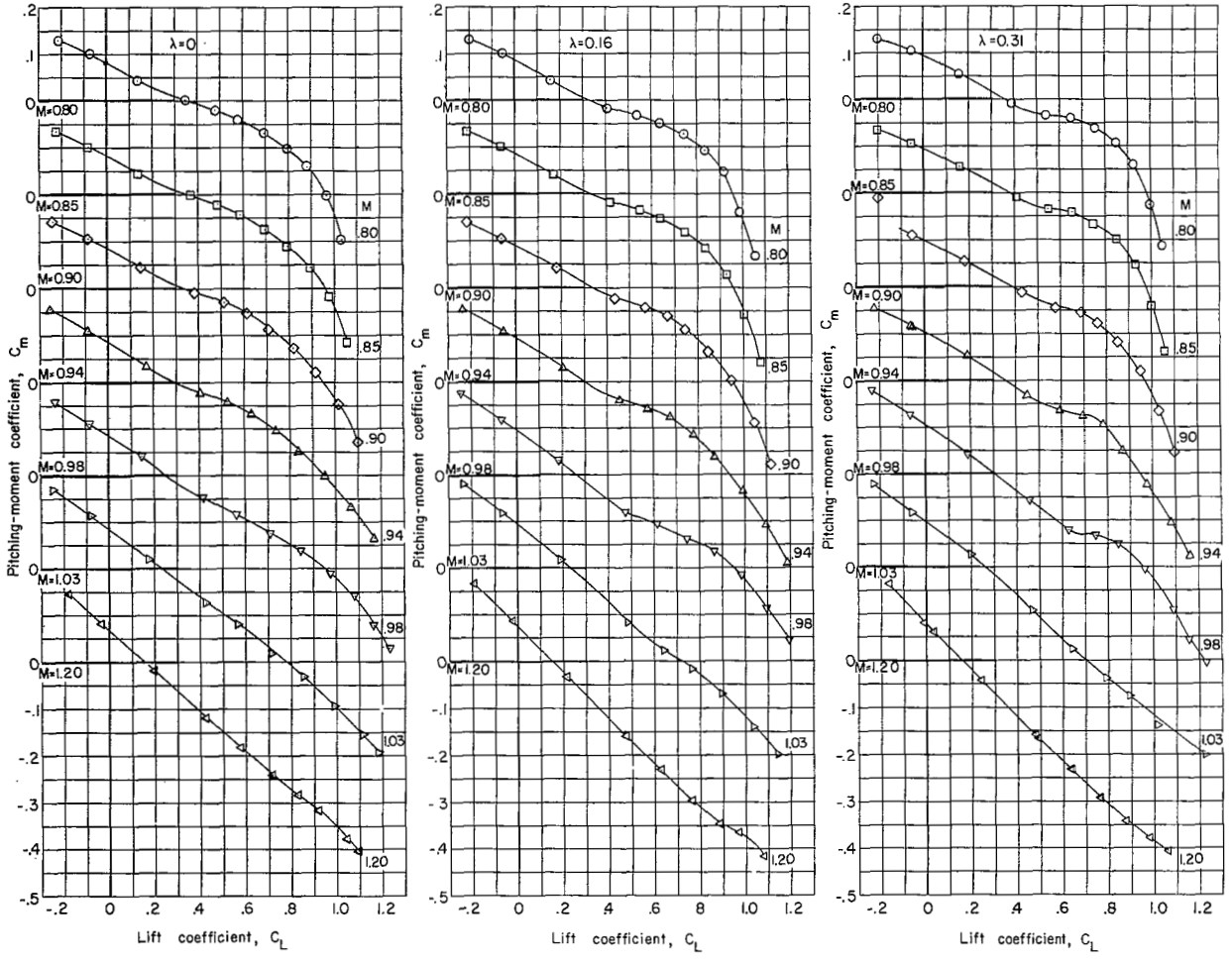

(a) Pitching moment.

Figure 7.- Aerodynamic characteristics of the wing-body-tail combinations; $i_t = -4^\circ$.

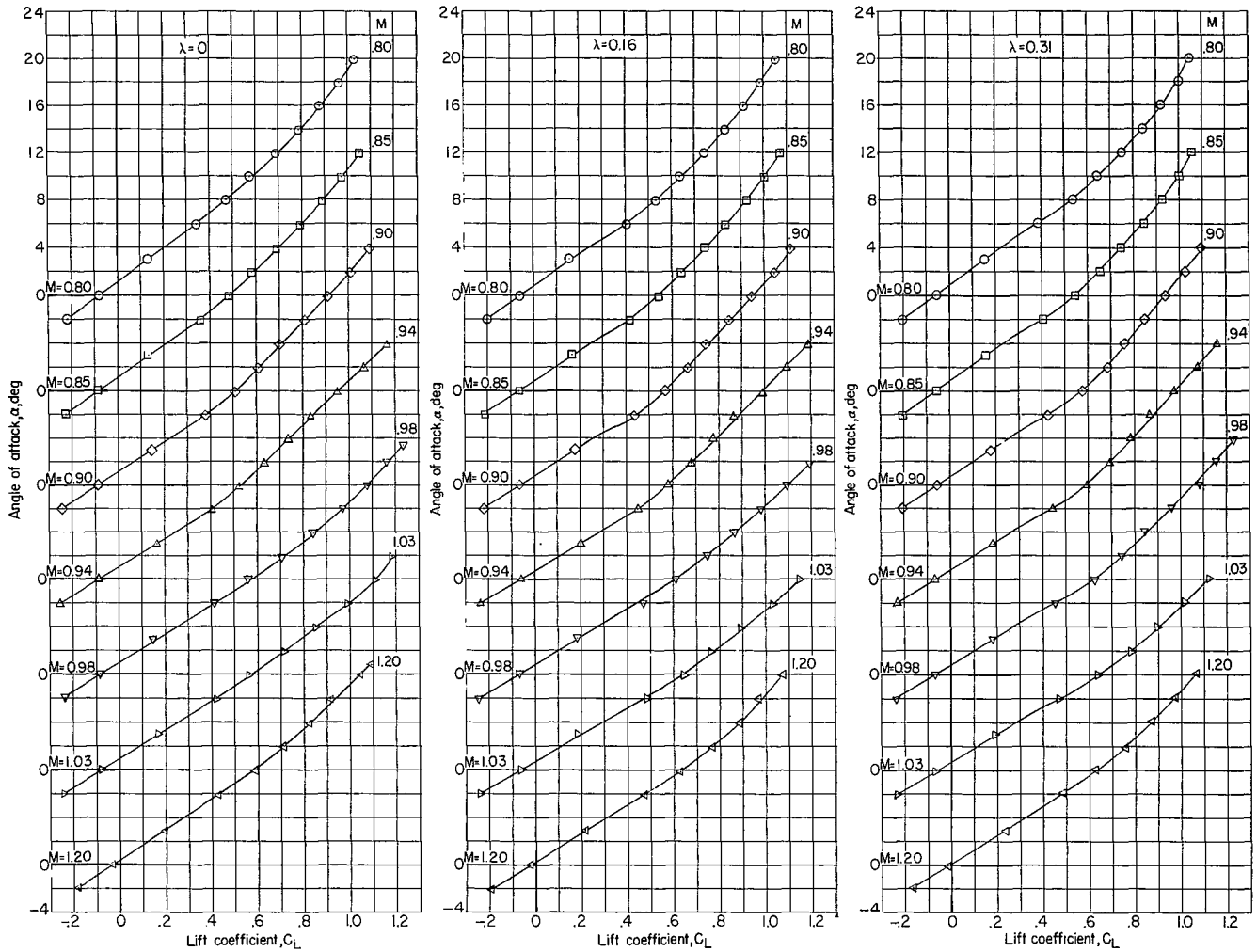

(b) Lift.

Figure 7.- Concluded.

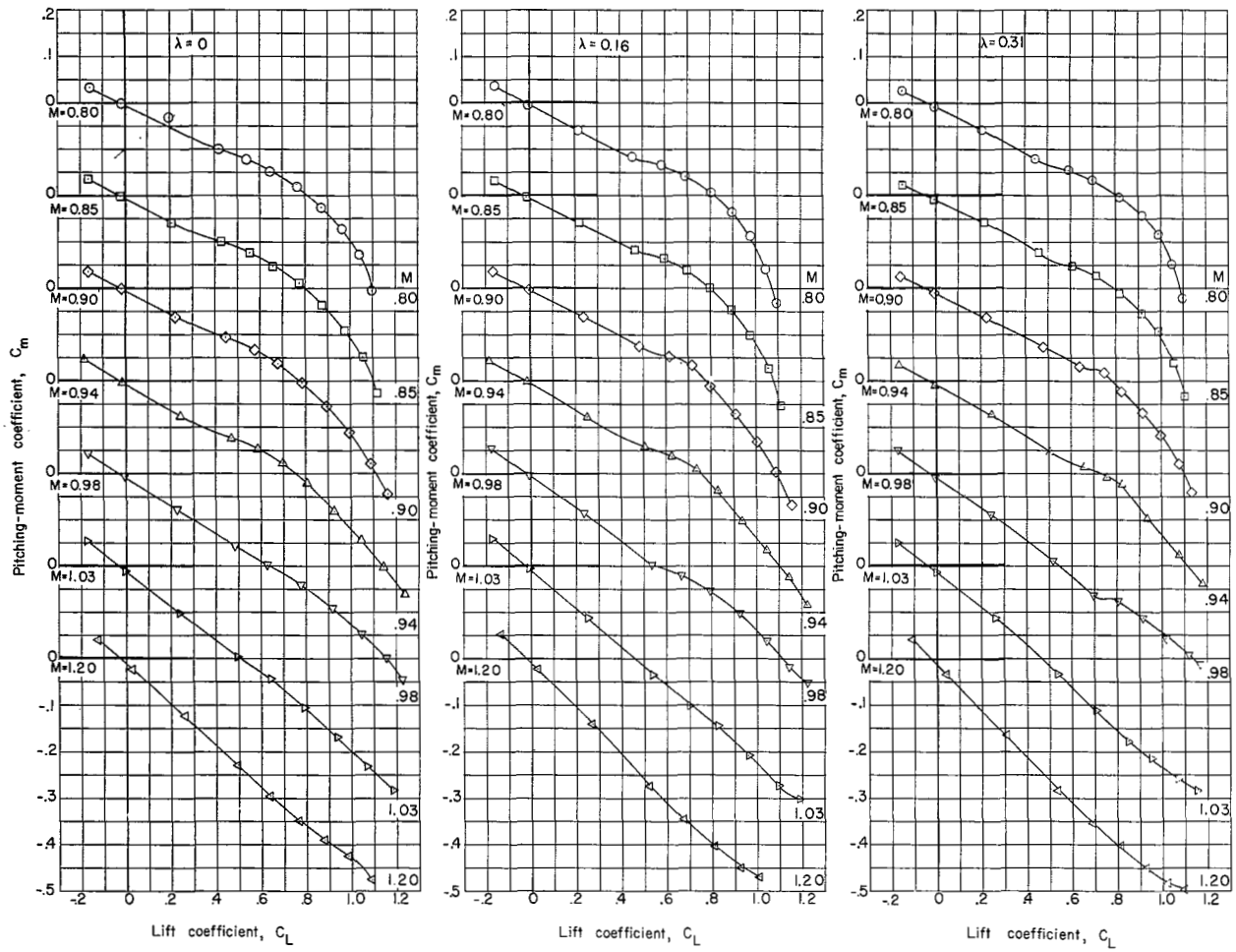

(a) Pitching moment.

Figure 8.- Aerodynamic characteristics of the wing-body-tail combination; $i_t = 0^\circ$.

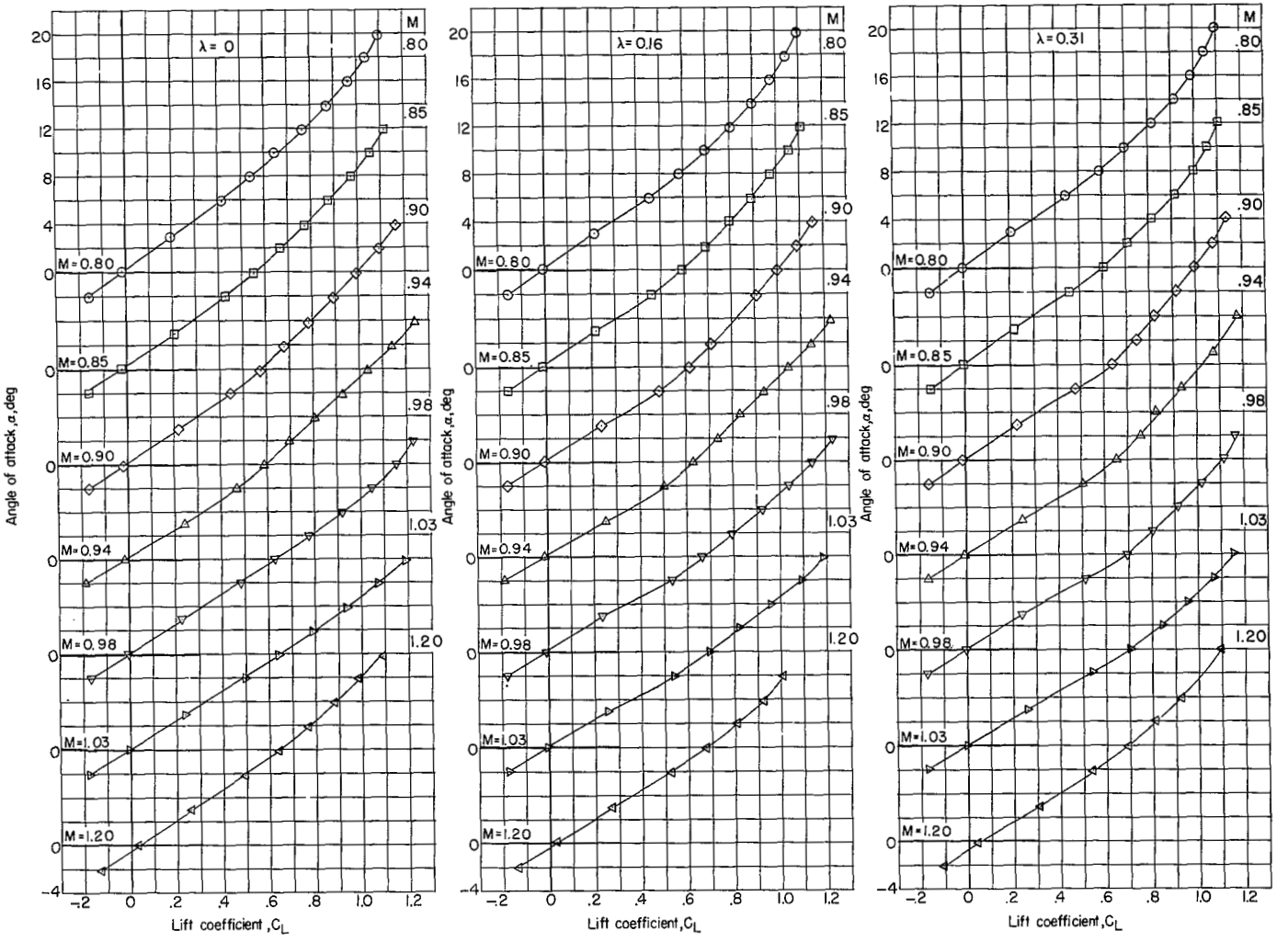

(b) Lift.

Figure 8.- Concluded.

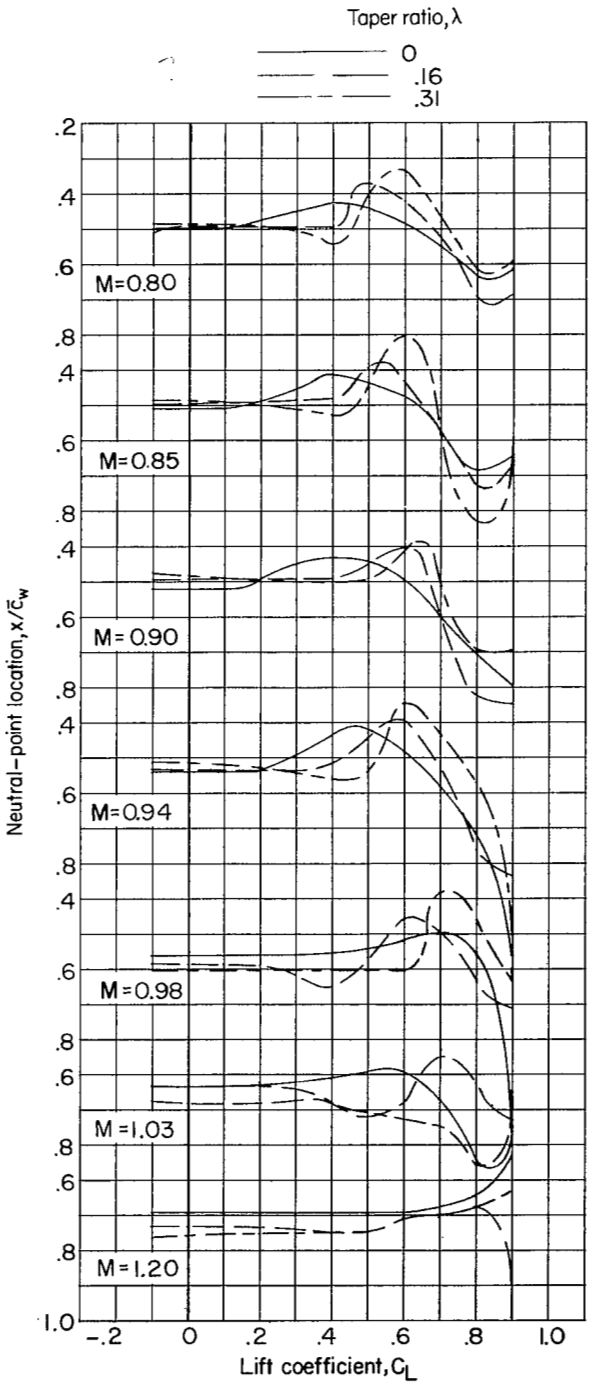

Figure 9.- Variation of neutral-point location with lift coefficient for the wing-body-tail combinations.

[redacted]

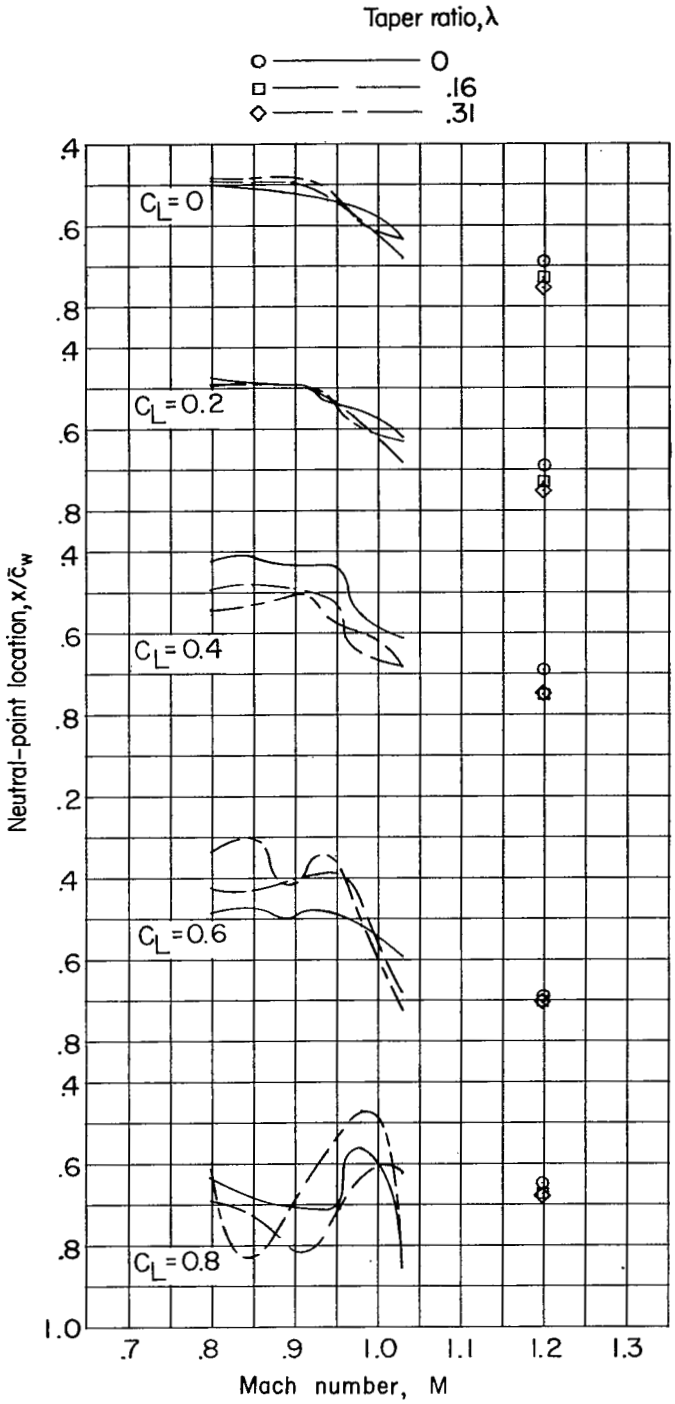

Figure 10.- Variation of neutral-point location with Mach number for the wing-body-tail combinations.

[redacted]

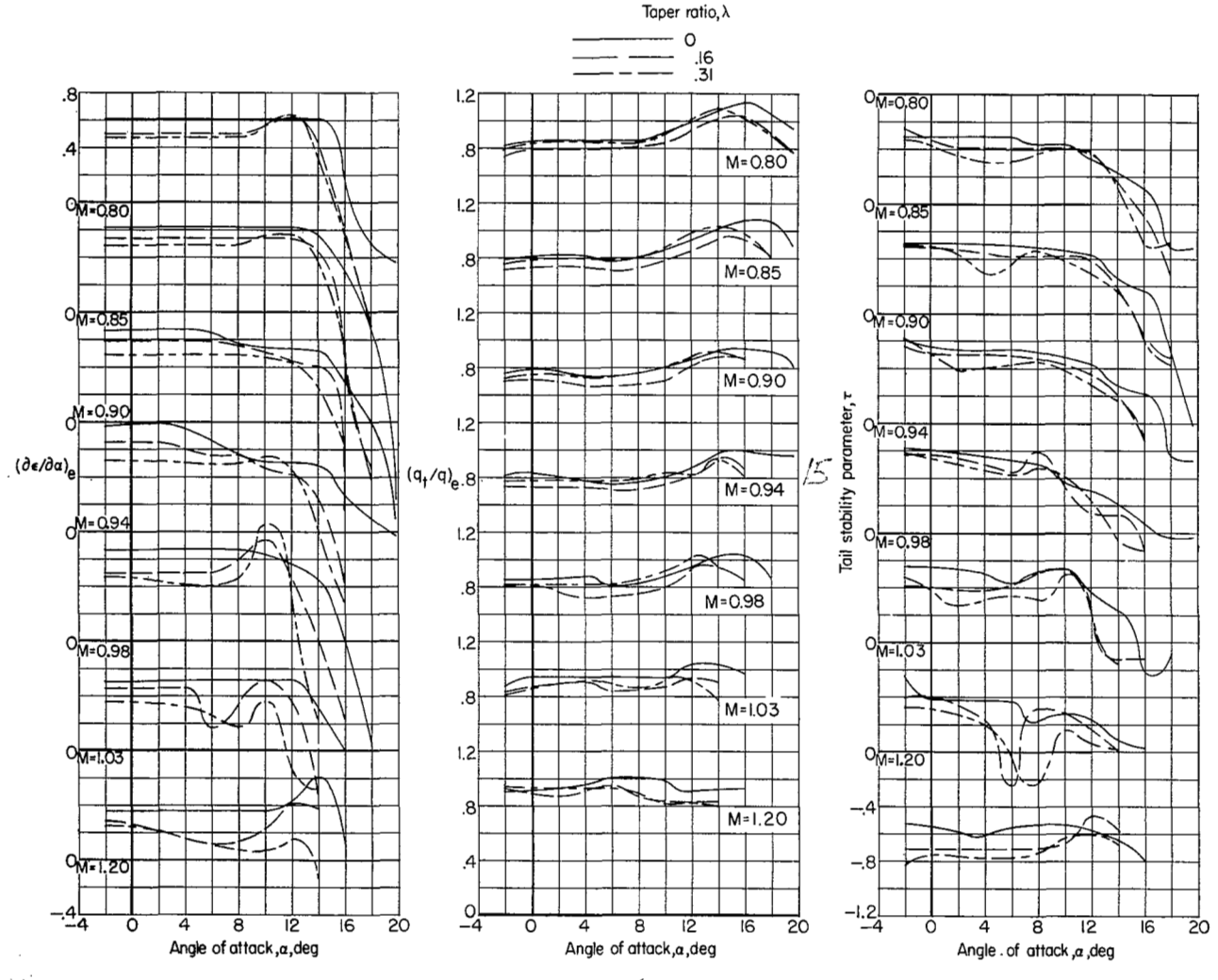

Figure 11.- Variation of parameters $(\partial\epsilon/\partial\alpha)_e$, $(q_t/q)_e$, and τ with angle of attack.

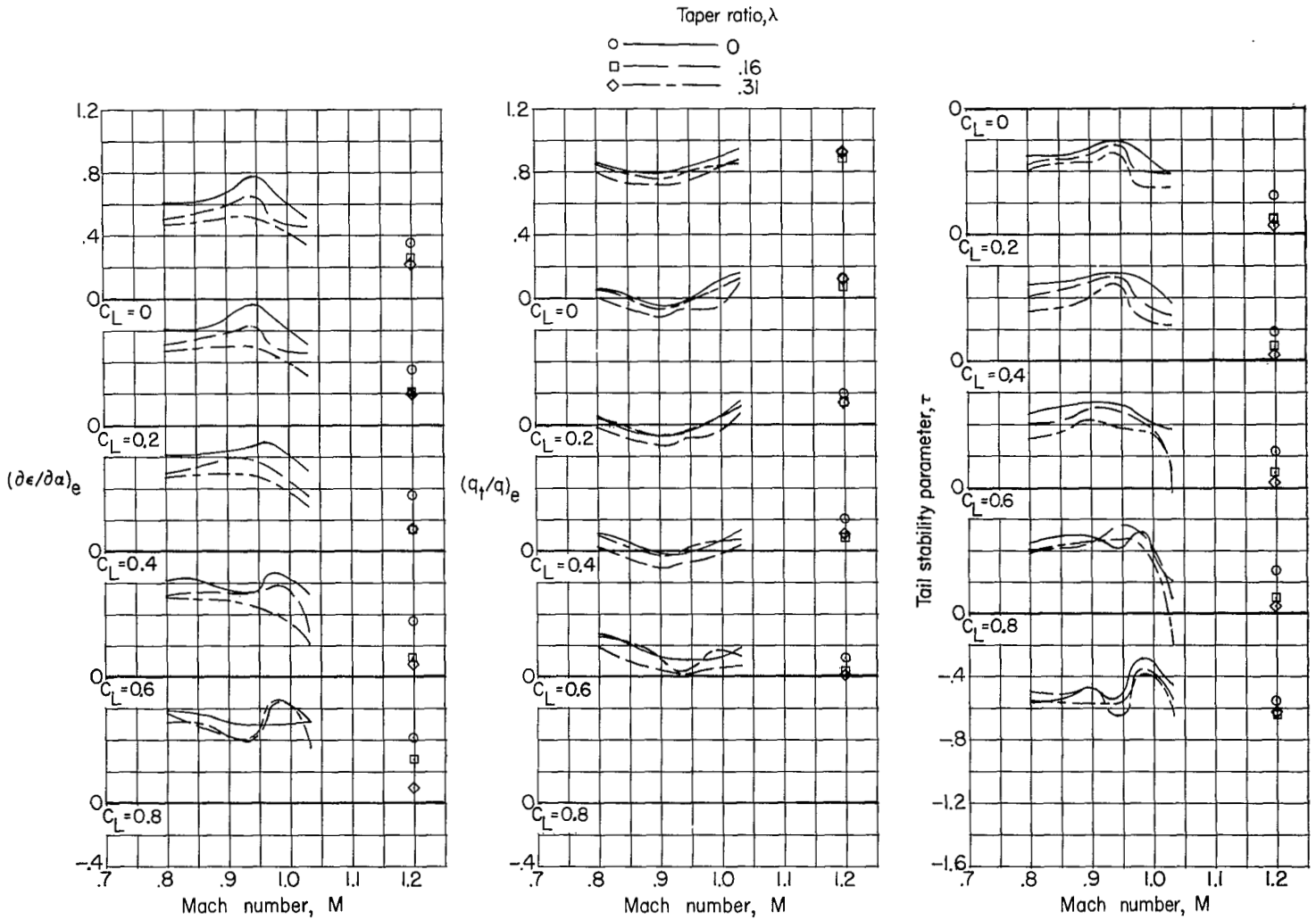

Figure 12.- Variation of parameters $(\partial\epsilon/\partial\alpha)_e$, $(q_t/q)_e$, and τ with Mach number.

NACA - Langley Field, Va.